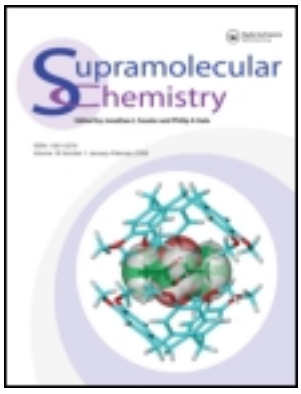

Supramolecular Chemistry
Publication details, including instructions for authors and subscription information:
http://www.tandfonline.com/loi/gsch20

Site-selective assembly between 1,8-diiodoperfluorooctane and 4,7,8,11-tetraazahelicene driven by halogen bonding

Serena Biella [a b], Massimo Cametti [a], Tullio Caronna [c], Gabriella Cavallo [a b], Alessandra Forni [d], Pierangelo Metrangolo [a b], Tullio Pilati [d], Giuseppe Resnati [a b d] & Giancarlo Terraneo [a b]

[a] NFMLab, DCMIC 'Giulio Natta', Politecnico di Milano, via Mancinelli 7, I-20131, Milan, Italy
[b] CNST-IIT@POLIMI, Politecnico di Milano, via Pascoli 70/3, I-20133, Milan, Italy
[c] Dipartimento di Ingegneria industriale, Università di Bergamo, viale Marconi 5, 24044, Dalmine, BG, Italy
[d] Institute of Molecular Science and Technology, CNR - University of Milan, via Golgi 19, I-20133, Milan, Italy

Available online: 13 Apr 2011

To cite this article: Serena Biella, Massimo Cametti, Tullio Caronna, Gabriella Cavallo, Alessandra Forni, Pierangelo Metrangolo, Tullio Pilati, Giuseppe Resnati & Giancarlo Terraneo (2011): Site-selective assembly between 1,8-diiodoperfluorooctane and 4,7,8,11-tetraazahelicene driven by halogen bonding, Supramolecular Chemistry, 23:03-04, 256-262

To link to this article: http://dx.doi.org/10.1080/10610278.2010.521841

Supramolecular Chemistry
Vol. 23, Nos. 3–4, March–April 2011, 256–262

Site-selective assembly between 1,8-diiodoperfluorooctane and 4,7,8,11-tetraazahelicene driven by halogen bonding

Serena Biella[ab], Massimo Cametti[a], Tullio Caronna[c], Gabriella Cavallo[ab], Alessandra Forni[d], Pierangelo Metrangolo[ab]*, Tullio Pilati[d], Giuseppe Resnati[abd]* and Giancarlo Terraneo[ab]

[a]*NFMLab, DCMIC 'Giulio Natta', Politecnico di Milano, via Mancinelli 7, I-20131 Milan, Italy;* [b]*CNST-IIT@POLIMI, Politecnico di Milano, via Pascoli 70/3, I-20133 Milan, Italy;* [c]*Dipartimento di Ingegneria industriale, Università di Bergamo, viale Marconi 5, 24044 Dalmine, BG, Italy;* [d]*Institute of Molecular Science and Technology, CNR – University of Milan, via Golgi 19, I-20133 Milan, Italy*

(*Received 28 July 2010; final version received 24 August 2010*)

The X-ray diffraction analysis on single crystals obtained from the self-assembly of 1,8-diiodoperfluorooctane **1** with the tetraazahelicene derivative **2** revealed a site-selective pattern of halogen bonds (XBs) in the solid state. Indeed, two non-equivalent XBs drive the formation of an indefinitely repeating pentameric $(\mathbf{1})_3{\cdot}(\mathbf{2})_2$ unit. Interestingly, the N···I—C bonding formation occurred selectively on the pyridazinic/cinnolinic nitrogen atoms of the tetraazahelicene unit, which were preferred over the pyridinic/quinolinic ones. On the basis of molecular electrostatic potential and molecular orbital analyses, DFT calculations predicted and explained well this site-selective XB formation, thus demonstrating to be efficient tools for the prediction of the XB site selectivity in similar polynitrogen systems.

Keywords: halogen bonding; diiodoperfluoroalkanes; azahelicenes; X-ray structure; DFT studies; molecular electronic potential; molecular orbital

1. Introduction

The search for materials endowed with novel properties is strategic for the development of technological applications, yet extremely challenging (*1*). One of the leading approaches to obtain new materials is self-assembly, which consists of the design of a set of components, i.e. molecular building blocks, which assemble each other in a controlled fashion due to their intrinsic structural and electronic properties (*2*). In order to achieve control over the desired architecture, non-covalent interactions, a broad category which encompasses forces of various nature, are used for gluing the molecular building blocks together. For this reason, non-covalent interactions are subjected to meticulous and continuous investigation by the scientific community (*3*). In fact, the precise understanding of such interactions is a fundamental prerequisite for the design of functional building blocks and for their full exploitation in material chemistry.

The polarisation effect exerted by strong electron-withdrawing groups renders a nearby halogen atom an excellent acceptor of electron density from an electron-rich donor. Such a type of interaction, disregarded only a few years ago, has been recently rediscovered and the term halogen bonding (XB) (*4*) has been introduced for describing any non-covalent interaction involving the positive region of the electrostatic potential surface of halogen atoms.[1] The general scheme D···X—Y thus applies to XB, wherein X is the halogen (Lewis acid, XB-donor), D is any electron donor (Lewis base, XB-acceptor) and Y is carbon, halogen, nitrogen, etc. The term XB itself sheds light on the nature of XB, which possesses numerous similarities with hydrogen bonding (HB), wherein hydrogen functions as the acceptor of electron density.

In the last decade or so, XBs have been thoroughly investigated in order to acquire insight on the physical determinants that cement together XB-donors and XB-acceptors (*5*). Generally, XB is considered to rely on a dominant electrostatic term, but other contributions are certainly present spanning from polarisation and dispersion forces to charge-transfer interactions. The iodine atom, given its lower electronegativity and larger polarisability in the halogen series, performs best as an XB-donor, provided that strong electron-withdrawing groups are present in close proximity to the halogen atom.

Among the various classes of molecules that can interact via XB, linear mono- and bis-iodo-perfluoroalkanes, i.e. the 1,8-diiodoperfluoroalkane **1** (Scheme 1), are among the most commonly employed XB-donors (*6*). Perfluorocarbon (PFC) residues are strongly electron withdrawing, and in addition, the $-(CF_2)_n-$ chain in a perfluoroalkane is significantly more stiff than the $-(CH_2)_n-$ chain in its hydrocarbon (HC) analogue and this confers an extra advantage in terms of preorganisation and structural control.

*Corresponding authors. Email: pierangelo.metrangolo@polimi.it; giuseppe.resnati@polimi.it

ISSN 1061-0278 print/ISSN 1029-0478 online

DOI: 10.1080/10610278.2010.521841
http://www.informaworld.com

Scheme 1. Molecular formulae of the XB-donor **1** and acceptors **2–4** mentioned in the text. Pyridinic/quinolinic nitrogen atoms are in blue, while the pyridazinic/cinnolinic ones are in red (colour online).

On the other hand, aromatic and aliphatic nitrogen-containing rings and their *N*-oxide derivatives function as XB-acceptors and have been effectively employed as building blocks for the self-assembly of various X-bonded supramolecular architectures (*4*). However, little is known on how to control selectivity among different electron donor sites in polynitrogen-containing heterocyclic systems. Recently, we reported an interesting case of site-selective supramolecular synthesis in X-bonded systems, wherein only the pyridinic nitrogen atoms of *trans*-4,4′-azobipyridine were involved in the recognition process (*7*). In order to increase the number of cases of site-selective XB formation in polynitrogen systems, we decided to undertake the study of the XB-acceptor behaviour of the tetraazahelicene derivative **2**, which presents both pyridinic/quinolinic and pyridazinic/cinnolinic nitrogen atoms (Scheme 1).

Helicenes belong to an intriguing class of polycyclic aromatic compounds that possess a characteristic helical conformation, responsible for their commonly used name (*8*), as well as a collection of interesting properties, such as large circular dichroism, long triplet lifetime, absorption at low-energy wavelength and tendency to give $\pi-\pi$ stacking. Helicenes are indeed promising molecular species for the development of light-emitting devices, sensors and non-linear optics (NLO)-active materials. The replacement of one or more carbon atoms with nitrogens, thus forming azahelicenes, may introduce the possibility for these molecules to be involved in site-specific intermolecular interactions while maintaining their properties and their distinctive helicity. For instance, monoazahelicenes have been already shown to be able to coordinate silver cations via quinolinic and isoquinolinic nitrogen atoms positioned in the internal rim of the helicenes, affording 2:1 (helicene/Ag^+) complexes in the solid state (*9*).

4,7,8,11-Tetraazahelicene **2** (Scheme 1), having two different sets of nitrogen atoms (pyridinic/quinolinic and pyridazinic/cinnolinic), is an ideal candidate to study the site selectivity of XB formation in polynitrogen aromatic systems. For the same reason, **2** was also selected as a good candidate for testing computational methods as tools for predicting the site selectivity of the XB, whenever a structural ambiguity is present. For all of these reasons, the molecular electrostatic potential (MEP) and molecular orbital (MO) analyses of the tetraazahelicene **2** were carried out by using DFT methods in order to predict the nitrogen sites that would have been involved in the XB formation following the co-crystallisation of **2** with the 1,8-diiodoperfluorooctane derivative **1** (Scheme 1).

2. Results and discussion

2.1 DFT calculations

Site-selective XBs have been already reported in several cases (*7*, *10*). The four nitrogen atoms of the tetraazahelicene **2** are all supposedly able to take part in strong XBs. While the proton affinity (and likewise gas phase basicity) of pyridine is greater than that of any of the diazines, regarding some weaker electron acceptors/Lewis acids (e.g. Li^+, Na^+ and K^+), both experimental measurements and theoretical calculations show pyridine to be a considerably weaker base than pyridazine (*11*). This relative tendency to function as donors of electron density of different azines is consistent with other reports on their acid/base behaviour and HB-acceptor ability (*12*). The two pyridazinic/cinnolinic nitrogen atoms on **2** were thus anticipated to function as preferred sites for the interaction with the XB-donor **1**. DFT calculations were prompted to provide more solid grounds to this hypothesis.

As previously highlighted, XB possesses a marked electrostatic character, similarly to HB (*13*). The MEP analysis, which gives information on what molecules 'see' when approaching one to the other, was thought to be extremely informative in order to ascertain the occurrence of a preferential attraction of the XB-donor **1** for either pyridinic/quinolinic or pyridazinic/cinnolinic nitrogen atoms on **2**, prior to establishing the actual interaction.

A plot of the MEP of **2** onto the surface of electron density with $\rho = 0.001$ a.u. is reported in Figure 1 (left). The MEP clearly indicates that the preferential sites for approaching the iodine atoms are located on the pyridazinic/cinnolinic nitrogen atoms, around which the largest and the deepest region of negative electrostatic potential (i.e. red region) is present. On the other hand,

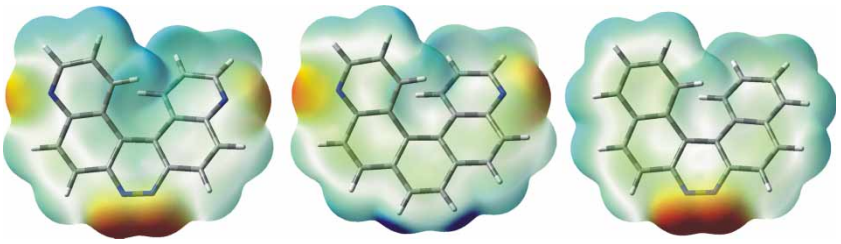

Figure 1. Plots of the B3LYP/6-311++G** electrostatic potential of compounds **2** (left), **3** (centre) and **4** (right) mapped on the respective isosurfaces (0.001 a.u.) of electron density. Minimum values of electrostatic potential are −0.0593 and −0.0447 a.u. (on pyridazinic/cinnolinic and pyridinic/quinolinic nitrogen atoms, respectively, of **2**), −0.0527 a.u. (**3**) and −0.0655 a.u. (**4**).

smaller and less negative regions of the MEP are located on the pyridinic/quinolinic nitrogen atoms, making them less suitable to attract the incoming diiodoperfluorinated module. For comparison, in Figure 1, the MEPs of the diazahelicenes **3** (centre) and **4** (right) are also reported. Both show slightly more negative values of the electrostatic potential around, respectively, the pyridinic/quinolinic and the pyridazinic/cinnolinic nitrogen atoms, with respect to the corresponding values obtained for **2**, indicating a mutual influence between the two sets of nitrogen atoms, when fused in a single polynitrogen heterocycle (*12*).

Further analysis was carried out on the nature of the frontier orbitals of the tetraazahelicene **2**, in particular the highest occupied MOs (HOMOs), in order to investigate the possibility of charge-transfer interactions directing, together with the electrostatic contribution addressed above, the establishment of the XB. Such an analysis (see Figure 2) revealed that the HOMO-1 (Figure 2, centre), which is almost degenerate with the HOMO, shows both larger contributions on the nitrogen atoms of the pyridazine moiety and the appropriate symmetry to interact with the incoming iodine atoms. The first MO with similar symmetry but showing larger contributions on the pyridine nitrogen atoms is HOMO-3 (Figure 2, right), which lies in energy well below the HOMO-1. The HOMO (Figure 2, left), while being delocalised over the full molecule, has nodal surfaces in correspondence of the four nitrogen atoms and therefore cannot be responsible for such interaction. In fact, according to a previous investigation aimed at determining the best frontier MOs responsible for a given reaction (*14*), the analysis of the composition and shape of the last occupied MO represents precisely the best criterion to identify such MOs, which does not necessarily coincide with the HOMO.

As expected, the combined results given by the MEP computation, altogether with the MO analysis, firmly indicate that the pyridazinic/cinnolinic nitrogen atoms on **2** are the preferential sites for the eventual acceptance of XBs in a given supramolecular system.

2.2 *X-ray diffraction analysis*

The evaporation at room temperature of a chloroform solution containing a 1:1 mixture of compounds **1** and **2**[2] yielded, after 1 day, good quality single crystals of composition $(\mathbf{1})_3\cdot(\mathbf{2})_2$, thus offering the opportunity for validating the prediction made by DFT calculations (see above). The single-crystal X-ray diffraction analysis revealed several interesting features. As shown in Figure 3, the observed XBs are established only with the pyridazinic/cinnolinic nitrogen atoms, as effectively predicted by the DFT calculations. Each of the two adjacent N atoms, in fact, interacts with two different diiodoperfluoroalkane modules making the tetraazahelicene to function as a bidentate XB-acceptor. The pyridinic/quinolinic nitrogen atoms, not involved in any XB, display, instead, weak H-bond interactions (N···H—C distances of 2.61 and 2.67 Å) with adjacent tetraazahelicenes (Figure 4).

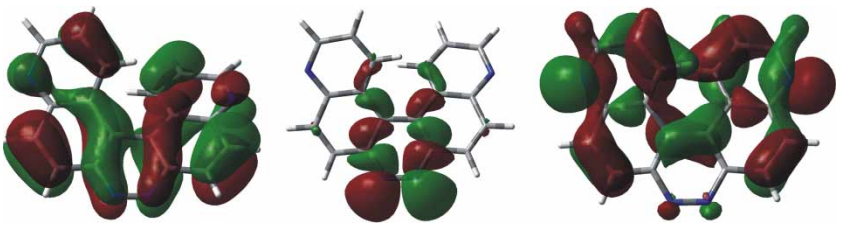

Figure 2. Surface plot of the B3LYP/6-311++G** HOMO (left), HOMO-1 (centre) and HOMO-3 (right) of the tetraazahelicene **2** (|isovalue| = 0.02 a.u.).

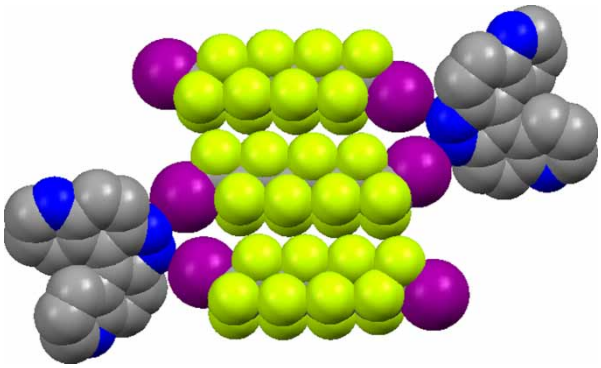

Figure 3. Spacefill representation of the XB-assembled pentamer $(\mathbf{1})_3{\cdot}(\mathbf{2})_2$ in the crystal (colour code: white, H; grey, C; blue, N; violet, I; yellow, F (colour online)).

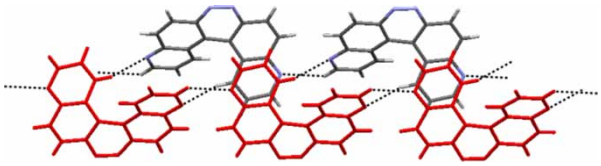

Figure 4. HB and π−π stacking motifs observed in the crystal structure (the second H-bonded layer of molecules of **2** is shown in red (colour online)).

Of the two X-bonded diiodoperfluorooctane molecules, one bridges two symmetry-related tetraazahelicenes, while the second one functions as a monodentate XB-donor. Hence, the overall XB-directed assembly, indefinitely repeated over the crystal lattice, is constituted by a pentameric, zigzag shaped, $(\mathbf{1})_3{\cdot}(\mathbf{2})_2$ adduct, i.e. two tetraazahelicenes and three diiodoperfluoroalkanes (Figure 3). Both the independent diiodoperfluorooctane molecules display the typical enantiomeric disorder of the PFC chains, whereas only the iodine atoms engaged in XB are ordered (*15*).

The two observed XBs are not equivalent. The linear bidentate XB-acceptor molecule experiences the shortest XB (N···I distance of 2.998 Å, while 168.3° is the mean N···I—C1(C,D) angle involving the two disordered C1C and C1D atoms), which lays on the pyridazinic/cinnolinic ring plane. Conversely, the other XB is significantly longer (distance 3.293 Å) with a less linear N···I—C1(A,B) angle (mean value 165.1°), consistent with a weaker XB taking place (*16*). This difference can be easily attributed to the vicinity of the two nitrogen atoms, which inhibits the formation of two geometrically ideal XBs, which would have resulted in the clashing of one of the two perfluorinated modules onto the other.

The X-bonded $(\mathbf{1})_3{\cdot}(\mathbf{2})_2$ pentamers are then tightly packed in the crystal lattice (no solvent molecules included), thanks to a cooperative set of various intermolecular interactions including HB, π−π stacking, and vdW and dispersion forces. In fact, besides the weak HB involving the pyridinic/quinolinic nitrogen atoms, the tetraazahelicene units are densely packed in an antiparallel fashion, showing π−π stacking between the external pyridinic/quinolinic rings that maximise dipole−dipole interactions (Figure 4).

It is worth to be reminded that PFC/HC interactions are generally very weak, and thus, phase separation is often observed in PFC/HC mixtures (*17*). XB is strong and specific enough to overcome this phase separation to the point of triggering the self-assembly of PFCs and HCs into hybrid co-crystals (*18*). In the system described in this paper, XB directs the self-assembly of the building blocks **1** and **2** into well-defined $(\mathbf{1})_3{\cdot}(\mathbf{2})_2$ pentamers. However, the packing of these pentamers is strongly reminiscent of the low affinity the starting materials have for each other, which results in the formation of segregated layers of perfluorinated and aromatic units, as commonly observed in similar systems (Figure 5).

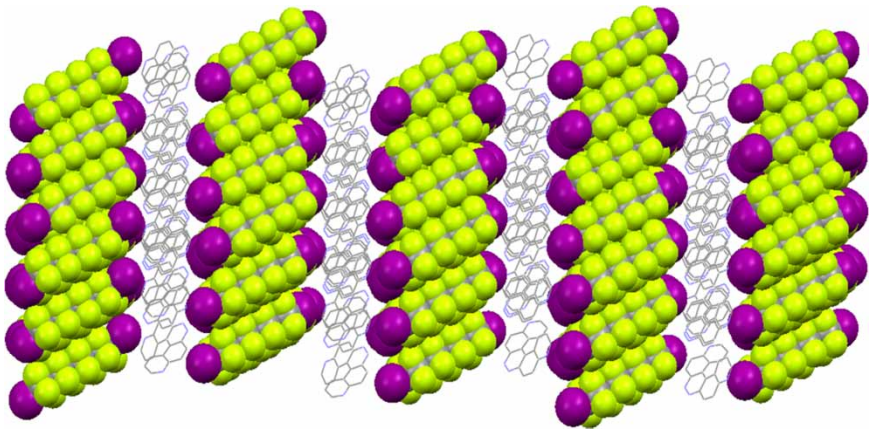

Figure 5. Representation of the segregation into layers in the lattice of the molecular components **1** (spacefill) and **2** (capped sticks).

3. Conclusions

In conclusion, this study shows that the tetraazahelicene **2** can be successfully used in the XB-mediated assembly of supramolecular architectures. Indeed, the self-assembly of the 1,8-diiodoperfluorooctane **1** with the tetraazahelicene **2** produced a lattice of packed pentameric units $(\mathbf{1})_3{\cdot}(\mathbf{2})_2$, the monomers of which are connected by two non-equivalent XBs. Interestingly, only the pyridazinic/cinnolinic nitrogen atoms were involved in the formation of XBs with the 1,8-diiodoperfluorooctane **1**, resulting in a site-selective supramolecular synthesis mediated by XB. This selectivity parallels the relative HB-basicity of the competing pyridinic/quinolinic and pyridazinic/cinnolinic nitrogen sites towards weaker Lewis acids. In this respect, XB shows the same selectivity found for HB in related polynitrogen heteroaromatics (*11*, *12*).

In the described pentameric system $(\mathbf{1})_3{\cdot}(\mathbf{2})_2$, the self-sorting process mediated by XB favours the modules' binding sites which allows for an optimal phase segregation between PFC and HC domains on the basis of thermodynamic considerations.

Little is known on how to predict and control selectivity among different supramolecular synthons. In the case reported in this article, DFT calculations were able to predict the observed site selectivity based on the analysis of both the electrostatic potential and the nature of the HOMOs of the tetraazahelicene **2**. These theoretical data suggest a twofold control, by electrostatic and charge-transfer interactions, on establishing of XB in this system, which selected the pyridazinic/cinnolinic atoms, over the pyridinic/quinolinic nitrogen atoms, as preferred sites for the XB formation with **1**. Such DFT approach has a general validity and, therefore, can be applied whenever the site selectivity of the XB in polynitrogen systems is of concern.

The results described in this article demonstrate that the tetraazahelicene **2** might be used as a new tecton in supramolecular chemistry capable of being involved into a twofold set of intermolecular interactions showing an orthogonal selectivity towards the two different sets of nitrogen atoms present onto **2**. Self-assembly processes using the tetraazahelicene **2** and based on simultaneous XB and HB, or XB and metal coordination, are currently in progress.

4. Experimental section

4.1 Synthesis

The synthesis of the tetraazahelicene **2** is an optimised version of the procedure reported by Huisgen (*25*). Compound **2**: ^{1}H NMR (250 MHz, $CDCl_3$): δ 9.11 (2H, dd, $J_1 = 1.5$ Hz, $J_2 = 4.2$ Hz), δ 9.00 (2H, d, $J = 8.75$ Hz), δ 8.84 (2H, d, $J = 9.25$ Hz), δ 8.50 (2H, d, $J = 9$ Hz), δ 7.42 (2H, m); ^{13}C NMR (63 MHz): δ 152.62, 149.74, 146.04, 136.07, 132.71, 130.80, 123.17, 120.12, 119.25; ESI mass: calcd for $C_{18}H_{10}N_4$ 282, found 283 $[M + H]^+$.

4.2 Crystal growth and X-ray diffraction

Single crystals were obtained by dissolving equimolar amounts of 1,8-diiodoperfluorooctane **1** and tetraazahelicene **2** at room temperature in a vial of clear borosilicate glass, using chloroform as a solvent. The open vial was introduced in a closed cylindrical glass jar containing paraffin oil. Chloroform was allowed to diffuse at room temperature, and after 1 day the formation of orange crystals was observed.

4.2.1 Complex $(\mathbf{1})_3{\cdot}(\mathbf{2})_2$

MF $= C_{60}H_{20}F_{48}I_6N_8$, FW $= 2526.24$, triclinic, space group P-1, $a = 9.897(2)$ Å, $b = 10.763(2)$ Å, $c = 20.010(3)$Å, $\alpha = 96.23(2)°$, $\beta = 90.90(2)°$, $\gamma = 116.07(2)°$, $V = 1898.5(6)$ Å^3, $Z = 1$, $D_x = 2.210$ mg m^{-3} and μ(Mo Kα) $= 2.618$ mm^{-1}; crystal dimensions $0.44 \times 0.26 \times 0.23$ mm^3, $\lambda = 0.71073$ Å (Mo Kα radiation), graphite monochromator, Bruker SMART-APEX CCD diffractometer. Data collection: ω and φ scan mode, $2\theta < 50°$; 10,790 collected reflections, 10,790 unique [6736 with $I_o > 2\sigma(I_o)$], merging $R = 0.02530$. The structure was solved by SIR2002 (*19*) and refined by SHELXL (*20*), full-matrix least squares based on F_o^2, with weights $w = 1/[\sigma^2(F_o)^2 + (0.0847P)^2]$, where $P = (F_o^2 + 2F_c^2)/3$. H atoms were in calculated positions. The final consistency index were $R = 0.0667$ and $Rw = 0.1488$ [0.0471 and 0.1403, respectively, for $I_o > 2\sigma(I_o)$], goodness of fit $= 1.029$. The final map ranges between -0.83 and 0.81 e Å^3. Detailed crystallographic data were deposited as CCDC 783798 with the Cambridge Crystallographic Data Centre, 12 Union Road, Cambridge CB2 1EZ, UK and can be obtained free of charge from http://www.ccdc.cam.ac.uk/products/csd/request/.

4.3 Computational details

Geometry optimisations of diazahelicenes and tetraazahelicenes were carried out in the gas phase with the Gaussian 03 software package (*21*) at the DFT (B3LYP) level (*22*), using the 6-311++G** basis set for all atoms. The basis set for iodine (*23*) was downloaded from the Basis Set Exchange site (*24*).

Acknowledgements

This work was funded by Fondazione Cariplo ('New-Generation Fluorinated Materials as Smart Reporter Agents in ^{19}F MRI') and MIUR ('Engineering of the Self-assembly of Molecular Functional Materials via Fluorous Interactions').

Notes

1. An IUPAC Task Group set up to examine the definition of halogen bonding has not yet reported, so that given here

should be taken as temporary (see www.iupac.org/web/ins/2009-032-1-100 and www.halogenbonding.eu).

2. The full characterisation of the molecular and supramolecular species reported in this article is given in Section 4 and in the Supporting Information, available online.

References

(1) Zhang, J.; Wojtas, L.; Larsen, R.W.; Eddaoudi, M.; Zaworotko, M.J. *J. Am. Chem. Soc*. **2009**, *131*, 17040–17041.

(2) Lehn, J.-M. *Supramolecular Chemistry: Concepts and Perspectives*; VCH: Weinheim, 1995; Hosseini, M.W. *Acc. Chem. Res.* **2005**, *38*, 313–323; Moulton, B.; Zaworotko, M.J. *Chem. Rev.* **2001**, *101*, 1629–1658.

(3) Lehn, J.-M. *Science* **2002**, *295*, 2400–2403; Reinhoudt, D.N.; Crego-Calama, M. *Science* **2002**, *295*, 2403–2407; Whitesides, G.M.; Mathias, J.P.; Seto, C.T. *Science* **1991**, *254*, 1312–1319; Müller-Dethlefs, K.; Hobza, P. *Chem. Rev.* **2000**, *100*, 143–168; Dougherty, D.A. *Science* **1996**, *271*, 163–168; Cockroft, S.L.; Hunter, C.A. *Chem. Commun.* **2006**, 3806–3808; Spitaleri, A.; Hunter, C.A.; McCabe, J.F.; Packer, M.J.; Cockroft, S.L. *CrystEngComm* **2004**, *6*, 490–494; Hunter, C.A.; Low, C.M.R.; Rotger, C.; Vinter, J.G.; Zonta, C. *Chem. Commun.* **2003**, 834–835; *Chem. Commun.* **2001**, 1500–1501.

(4) Bertani, R.; Sgarbossa, P.; Venzo, A.; Lelj, F.; Amati, M.; Resnati, G.; Pilati, T.; Metrangolo, P.; Terraneo, G. *Coord. Chem. Rev.* **2010**, *254*, 677–695; Roper, L.C.; Präsang, C.; Kozhevnikov, V.N.; Whitwood, A.C.; Karadakov, P.B.; Bruce, D.W. *Cryst. Growth Des.* **2010**, *10*, 3710–3720; Raatikainen, K.; Rissanen, K. *Cryst. Growth Des.* **2010**, *10*, 3638–3646; Raatikainen K.; Rissanen, K. *CrystEngComm* **2009**, *11*, 750–752; Raatikainen, K.; Huuskonen, J.; Lahtinen, M.; Metrangolo, P.; Rissanen, K. *Chem. Commun.* **2009**, 2160–2162; Metrangolo, P.; Pilati, T.; Terraneo, G.; Biella, S.; Resnati, G. *CrystEngComm* **2009**, *11*, 1187–1196; Metrangolo, P.; Resnati, G. *Science* **2008**, *321*, 918–919; Rissanen, K. *CrystEngComm* **2008**, *10*, 1107–1113; Metrangolo, P.; Neurkirch, H.; Pilati, T.; Resnati, G. *Acc. Chem. Res.* **2005**, *38*, 386–395; Amico, V.; Bertani, R.; Metrangolo, P.; Moiana, A.; Perez, E.; Pilati, T.; Resnati, G.; Rico-Lattes, I.; Sassi, A. *Adv. Mater.* **2002**, *14*, 1197–1201; Metrangolo, P.; Resnati, G. *Chem. Eur. J.* **2001**, *7*, 2511–2519; Walsh, R.B.; Padgett, C.W.; Metrangolo, P.; Resnati, G.; Hanks, T.W.; Pennington, W.T. *Cryst. Growth Des.* **2001**, *1*, 165–175; Cardillo, P.; Corradi, E.; Lunghi A.; Meille, S.V.; Messina, M.T.; Metrangolo, P.; Resnati, G. *Tetrahedron* **2000**, *56*, 5535–5550; Corradi, E.; Meille, S.V.; Messina, M.T.; Metrangolo, P.; Resnati, G. *Angew. Chem.* **2000**, *112*, 1852–1856; Corradi, E.; Meille, S.V.; Messina, M.T.; Metrangolo, P.; Resnati, G. *Angew. Chem. Int. Ed.* **2000**, *39*, 1782–1786; Corradi, E.; Meille, S.V.; Messina, M.T.; Metrangolo, P.; Resnati, G. *Tetrahedron Lett.* **1999**, *40*, 7519–7523; Meille, S.V.; Corradi, E.; Messina, M.T.; Resnati, G. *J. Am. Chem. Soc.* **1998**, *120*, 8261–8262.

(5) Cabot, R.; Hunter, C. *Chem. Commun.* **2009**, 2005–2007; Wang, W.; Hobza, P. *J. Phys. Chem. A* **2008**, *112*, 4114–4119; Zou, J.-W.; Jiang, Y.-J; Guo, M.; Hu, G.-X.; Zhang, B.; Liu, H.-C.; Yu, Q.S. *Chem. Eur. J.* **2005**, *11*, 740–751; Ananthavel, S.P.; Manoharan, M. *Chem. Phys.* **2001**, *269*, 49–57; Politzer, P.; Lane, P.; Concha, M.C; Ma, Y.; Murray, J.S. *J. Mol. Model.* **2007**, *13*, 305–311; Clark, T.; Hennemann, M.; Murray, J.S.; Politzer, P. *J. Mol. Model.* **2007**, *13*, 291–296; Awwadi, F.F.; Willett, R.D.; Peterson, K.A; Twamley, B. *Chem. Eur. J.* **2006**, *12*, 8952–8960.

(6) Fan, H.; Eliason, J.K.; Moliva, A.C.D.; Olson, J.L.; Flancher, S.M.; Gealy, M.W.; Ulness, D.J. *J. Phys. Chem. A* **2009**, *113*, 14052–14059; Metrangolo, P.; Carcenac, Y.; Lahtinen, M.; Pilati, T.; Rissanen, K.; Vij, A.; Resnati, G. *Science* **2009**, *323*, 1461–1464; Casnati, A.; Cavallo, G.; Metrangolo, P.; Resnati, G.; Ugozzoli, F.; Ungaro, R. *Chem. Eur. J*. **2009**, *15*, 7903–7912; Metrangolo, P.; Meyer, F.; Pilati, P.; Proserpio, D.M.; Resnati, G. *Chem. Eur. J.* **2007**, *13*, 5765–5772; Fox, D.B.; Liantonio, R.; Metrangolo, P.; Pilati, T.; Resnati, G. *J. Fluor. Chem.* **2004**, *125*, 271–281; Liantonio, R.; Metrangolo, P.; Pilati, T.; Resnati, G.; Stevenazzi, A. *Cryst. Growth Des.* **2003**, *3*, 799–803; Navarrini, W.; Metrangolo, P.; Pilati, T.; Resnati, G. *New J. Chem*. **2000**, *24*, 777–780.

(7) Fox, D.; Metrangolo, P.; Pasini, D.; Pilati, T.; Resnati, G.; Terraneo, G. *CrystEngComm* **2008**, *10*, 1132–1136.

(8) Martin, R.H. *Angew. Chem.* **1974**, 727–738; Katz, T.J. *Angew. Chem.* **2000**, *112*, 1997–1999; *Angew. Chem. Int. Ed.* **2000**, *39*, 1921–1923; Grimme, S.; Harren, J.; Sobanski, A.; Vögtle, F. *Eur. J. Org. Chem.* **1998**, *8*, 1491–1509; Passeri, R.; Gaetano Aloisi, G.; Elisei, F.; Latterini, L.; Caronna, T.; Fontana, F.; Natali Sora, I. *Photochem. Photobiol. Sci.* **2009**, *8*, 1574–1582; Wigglesworth, T.J.; Sud, D.; Norsten, T.B.; Lekhi, V.S.; Branda, N.R. *J. Am. Chem. Soc.* **2005**, *127*, 7272–7273; Reetz, M.T.; Sostmann, S. *Tetrahedron* **2001**, *55*, 2515–2520; Field, J.E.; Muller, G.; Riehl, J.P.; Venkataraman, D. *J. Am. Chem. Soc.* **2005**, *125*, 11808–11809; Hassey, R.; Swain, E.J.; Hammer, N.I.; Venkataraman, D.; Barnes, M.D. *Science* **2006**, *314*, 1437–1439; Verbiest, T.; Van Elsocht, S.; Kauranen, M.; Hellemans, L.; Snauwaert, J.; Nuckolls, C.; Katz, T.J.; Persoons, A. *Science* **1998**, *282*, 913–915; Verbiest, T.; Sioncke, S.; Persoons, A.; Vylicky, L.; Katz, T.J. *Angew. Chem. Int. Ed.* **2002**, *41*, 3882–3884; Furche, F.; Ahlrichs, R.; Wacksmann, C.; Weber, E.; Sobanski, A.; Vögtle, F.; Grimme, S. *J. Am. Chem. Soc.* **2000**, *122*, 1717–1724; Autschbach, J.; Ziegler, T.; van Gisbergen, S.J.A.; Baerends, E.J. *J. Chem. Phys*. **2002**, *116*, 6930–6940; Spassova, M.; Asselberghs, I.; Verbiest, T.; Clays, K.; Botek, E.; Champagne, B. *Chem. Phys. Lett*. **2007**, *439*, 213–218; Champagne, B.; André, J.M.; Botek, E.; Licandro, E.; Maiorana, S.; Bossi, A.; Clays, K.; Persoons, A. *Chem. Phys. Chem.* **2004**, *5*, 1438–1442.

(9) Misek, J.; Teply, F.; Stara, I.G.; Tichy, M.; Saman, D.; Cisarova, I.; Vojtisek, P.; Stary, I. *Angew. Chem. Int. Ed.* **2008**, *47*, 3188–3191.

(10) Bruce, D.W.; Metrangolo, P.; Meyer, F.; Pilati, T.; Präsang, C.; Resnati, G.; Terraneo, G.; Wainwright, S.G.; Whitwood, A.C. *Chem. Eur. J.* **2010**, *16*, 9511–9524; Lapadula, G.; Judaš, N.; Friščić, T.; Jones, W. *Chem. Eur. J.* **2010**, *16*, 7400–7403; Metrangolo, P.; Meyer, F.; Pilati, T.; Proserpio, D.M.; Resnati, G. *Chem. Eur. J.* **2007**, *13*, 5765–5772; Metrangolo, P.; Präsang, C.; Resnati, G.; Liantonio, R.; Whitwood, A.C.; Bruce, D.W. *Chem. Commun.* **2006**, 3290–3292; Syssa-Magalé, J.-L.; Boubekeur, K.; Palvadeau, P.; Meerschaut, A.; Schöllhorn, B.; *CrystEngComm* **2005**, *7*, 302–308; Syssa-Magalé, J.-L.; Boubekeur, K.; Schöllhorn, B. *J. Mol. Struct.* **2005**, *737*, 103–107; Amico, V.; Meille, S.V.; Corradi, E.; Messina, M.T.; Resnati, G. *J. Am. Chem. Soc.* **1998**, *120*, 8261–8262.

(11) Lipkind, D.; Chickos, J.S.; Liebman, J.F. *Struct. Chem.* **2009**, *20*, 617–618.

(12) Berthelot, M.; Laurence, C.; Safar, M.; Besseau, F. *J. Chem. Soc., Perkin Trans. 2* **1998**, 283–290.
(13) Bianchi, R.; Forni, A.; Pilati, T. *Chem. Eur. J.* **2003**, *9*, 1631–1638; Bianchi, R.; Forni, A.; Pilati, T. *Acta Crystallogr. Sect. B* **2004**, *60*, 559–568; Forni, A. *J. Chem. Phys. A* **2009**, *113*, 3403–3412.
(14) Da Silva, R.R.; Ramalho, T.C.; Santos, J.M.; Figueroa-Villar, J.D. *J. Phys. Chem. A* **2006**, *110*, 1031–1040 and references cited therein.
(15) Dey, A.; Metrangolo, P.; Pilati, T.; Resnati, G.; Terraneo, G.; Wlassics, I. *J. Fluor. Chem.* **2009**, *130*, 816–823.
(16) The sum of the VdW radii for N (155 pm) and I (198 pm) is 353 pm. See Bondi, A. *J. Phys. Chem.* **1964**, *68*, 441–451.
(17) Smart, B.E. *J. Fluor. Chem.* **2001**, *109*, 3–11.
(18) Metrangolo, P.; Pilati, T.; Resnati, G.; Stevanazzi, A. *Curr. Opin. Colloid Interface Sci.* **2003**, *8*, 215–222.
(19) Burla, M.C.; Camalli, M.; Carrozzini, B.; Cascarano, G.L.; Giacovazzo, C.; Polidori, G.; Spagna, R. *J. Appl. Cryst.* **2003**, *36*, 1103.
(20) Sheldrick, G.M. *Acta Cryst.* **2008**, *A64*, 112–122.
(21) Frisch, M.J.; Trucks, G.W.; Schlegel, H.B.; Scuseria, G.E.; Robb, M.A.; Cheeseman, J.R.; Montgomery, J.A., Jr.; Vreven, T.; Kudin, K.N.; Burant, J.C.; Millam, J.M.; Iyengar, S.S.; Tomasi, J.; Barone, V.; Mennucci, B.; Cossi, M.; Scalmani, G.; Rega, N.; Petersson, G.A.; Nakatsuji, H.; Hada, M.; Ehara, M.; Toyota, K.; Fukuda, R.; Hasegawa, J.; Ishida, M.; Nakajima, T.; Honda, Y.; Kitao, O.; Nakai, H.; Klene, M.; Li, X.; Knox, J.E.; Hratchian, H.P.; Cross, J.B.; Bakken, V.; Adamo, C.; Jaramillo, J.; Gomperts, R.; Stratmann, R.E.; Yazyev, O.; Austin, A.J.; Cammi, R.; Pomelli, C.; Ochterski, J.W.; Ayala, P.Y.; Morokuma, K.; Voth, G.A.; Salvador, P.; Dannenberg, J.J.; Zakrzewski, V.G.; Dapprich, S.; Daniels, A.D.; Strain, M.C.; Farkas, O.; Malick, D.K.; Rabuck, A.D.; Raghavachari, K.; Foresman, J.B.; Ortiz, J.V.; Cui, Q.; Baboul, A.G.; Clifford, S.; Cioslowski, J.; Stefanov, B.B.; Liu, G.; Liashenko, A.; Piskorz, P.; Komaromi, I.; Martin, R.L.; Fox, D.J.; Keith, T.; Al-Laham, M.A.; Peng, C.Y.; Nanayakkara, A.; Challacombe, M.; Gill, P.M.W.; Johnson, B.; Chen, W.; Wong, M.W.; Gonzalez, C.; Pople, J.A. *Gaussian 03, Revision C.02*; Gaussian, Inc.: Wallingford CT, 2004.
(22) Becke, A.D. *J. Chem. Phys.* **1993**, *98*, 5648–5652; Lee, C.; Yang, W.; Parr, R.G. *Phys. Rev. B: Condens. Matter* **1988**, *37*, 785–789.
(23) Glukhovstev, M.N.; Pross, A.; McGrath, M.P.; Radom, L. *J. Chem. Phys.* **1995**, *103*, 1878–1885.
(24) Feller, D. *J. Comp. Chem.* **1996**, *17*, 1571–1586; Schuchardt, K.L.; Didier, B.T.; Elsethagen, T.; Sun, L.; Gurumoorthi, V.; Chase, J.; Li, J.; Windus, T.L. *J. Chem. Inf. Model.* **2007**, *47*, 1045–1052.
(25) Huisgen, R. *Justus Liebigs Annalen der Chemie* **1948**, *559*, 101–152.